From Rolling Ball to Complete Wetting: The Dynamic Tuning of Liquids on Nanostructured Surfaces

Tom N. Krupenkin,* J. Ashley Taylor, Tobias M. Schneider, and Shu Yang

Bell Laboratories, Lucent Technologies, 600-700 Mountain Avenue, Murray Hill, New Jersey 07974

Received November 6, 2003. In Final Form: January 8, 2004

In this work, for the first time, a dynamic electrical control of the wetting behavior of liquids on nanostructured surfaces, which spans the entire possible range from the superhydrophobic behavior to nearly complete wetting, has been demonstrated. Moreover, this kind of dynamic control was obtained at voltages as low as 22 V. We have demonstrated that the liquid droplet on a nanostructured surface exhibits sharp transitions between three possible wetting states as a function of applied voltage and liquid surface tension. We have examined experimentally and theoretically the nature of these transitions. The reported results provide novel methods of manipulating liquids at the microscale.

Introduction

It has been known for a long time[1,2] that a high degree of surface roughness often results in a substantial increase in the degree of hydrophobicity of the solid substrate. More recently,[3−17] this phenomenon, coupled with the modern self-assembly and microfabrication techniques, has been used to demonstrate so-called superhydrophobic surfaces, which exhibit a number of new and exciting properties such as extremely high contact angles and very low flow resistance. This kind of behavior makes the superhydrophobic surfaces important candidates for a wide range of applications, from microfluidics and lab-on-a-chip devices to drag reduction and self-cleaning coatings.

Although some results on dynamically tunable regular surfaces were recently reported,[18,19] up to now, there was no effective way to dynamically tune the properties of superhydrophobic surfaces. At the same time, in many applications it would be highly advantageous to be able to dynamically adjust the behavior of liquids on the superhydrophobic surfaces, including the droplet mobility, contact angle, and effective area of the solid−liquid interface. Such level of control would potentially allow novel methods of manipulating liquids at both the micro- and the macroscales. One of the promising ways to achieve this goal is to employ the electrowetting effect. It has been known for some time that electrowetting can be successfully used to dynamically adjust the effective energy of the solid−liquid interfaces.[20−30] However, it is not easy to achieve effective electrowetting on most of the existing superhydrophobic surfaces using the traditional electrowetting setup,[22−30] where the voltage is applied between the liquid droplet and the electrode positioned at some distance beneath the dielectric solid surface. One problem is the high degree of roughness exhibited by superhydrophobic surfaces, which causes substantial spatial separation between the liquid and the underlying electrode, strongly impeding the electrowetting effect.

In this work, we propose a new approach that allows us to achieve effective electrowetting on nanostructured superhydrophobic surfaces. We have demonstrated, for the first time, that electrowetting can be effectively used to dynamically change the way liquids wet nanostructured surfaces covering the widest possible range, from strong superhydrophobic behavior to nearly complete wetting. We have also demonstrated that this change is accompanied by a dramatic increase in the effective area of the liquid−solid interface and, thus, by a strong decrease

* Author to whom correspondence should be addressed. E-mail: tnk@lucent.com.

(1) Wenzel, R. N. *J. Phys. Colloid Chem.* **1949**, *53*, 1466.
(2) Cassie, A. B. D.; Baxter, S. *Trans. Faraday Soc.* **1944**, *40*, 546.
(3) Shibuichi, S.; Onda, T.; Satoh, N.; Tsujii, K. *J. Phys. Chem.* **1996**, *100*, 19512.
(4) Miwa, M.; Nacajima, A.; Fujishima, A.; Hashimoto, K.; Watanabe, T. *Langmuir* **2000**, *16*, 5754.
(5) Chen, W.; Fadeev, A. Y.; Hsieh, M. C.; Öner, D.; Youngblood, J.; McCarthy, T. J. *Langmuir* **1999**, *15*, 3395.
(6) Torkkeli, A.; Saarilahti, J.; Häärä, A.; Härmä, H.; Soukka, T.; Tolonen, P. Electrostatic transportation of water droplets on superhydrophobic surfaces. *Proc. IEEE Micro Electro Mech. Syst.* **2001**, 475−478.
(7) Youngblood, J. P.; McCarthy, T. J. *Macromolecules* **1999**, *32*, 6800.
(8) Inoue, Y.; Yoshimura, Y.; Ikeda, Y.; Kohno, A. *Colloids Surf., B* **2000**, *19*, 257.
(9) Matsumoto. Y.; Ishida, M. *Sens. Actuators* **2000**, *83*, 179.
(10) Hozumi, A.; Takai, O. *Thin Solid Films* **1997**, *303*, 222.
(11) Bico, J.; Marzolin, C.; Quéré, D. *Europhys. Lett.* **1999**, *47*, 220.
(12) Nakejima, A.; Hashimoto, K.; Watanabe, T. *Monatsh. Chem.* **2001**, *132*, 31.
(13) Kim, J.; Kim, C. J. Nanostructured surfaces for dramatic reduction of flow resistance in droplet-based microfluidics. *Proc. IEEE Micro Electro Mech. Syst.* **2002**, 479−482.
(14) Bico, J.; Tordeux, C.; Quere, D. *Europhys. Lett.* **2001**, *55*, 214.
(15) Patankar, N. *Langmuir* **2003**, *19*, 1249.
(16) Lafuma, A.; Quere, D. *Nat. Mater.* **2003**, *2*, 457.
(17) Krupenkin, T.; Kornblit, A.; Schneider, T. M.; Taylor, J. A.; Mandich, M.; Yang, S. Method And Apparatus For Variably Controlling The Movement Of A Liquid On A Nanostructured Surface. U.S. Patent Application 10,403,159, March 31, 2003.
(18) Ichimura, K.; Oh, S.-K.; Nakagawa, M. *Science* **2000**, *288*, 1624.
(19) Lahann, J.; Mitragotri, S.; Tran, T.-N.; Kaido, H.; Sundaram, J.; Choi, I. S.; Hoffer, S.; Somorjai, G.; Langer, R. *Science* **2003**, *299*, 371.
(20) Minnema, L.; Barnevald, H. A.; Rinkel, P. D. *IEEE Trans. Electr. Insul.* **1980**, *E1−15*, 461.
(21) Beni, G.; Hackwood, S. *Appl. Phys. Lett.* **1980**, *38*, 207.
(22) Verheijen, H. J. J.; Prins, M. W. J. *Langmuir* **1999**, *15*, 6616.
(23) Seyrat, E.; Hayes, R. A. *J. Appl. Phys.* **2001**, *90*, 1383.
(24) Moon, H.; Cho, S. K.; Garrell, R. L.; Kim, C. J. *J. Appl. Phys.* **2002**, *92*, 4080.
(25) Pollack, M. G.; Fair, R. B.; Shenderov, A. D. *Appl. Phys. Lett.* **2000**, *77*, 1725.
(26) Cho, S. K.; Fan, S. K.; Moon, H.; Kim, C. J. Towards Digital Microfluidic Circuits: Creating, Transporting, Cutting and Merging Liquid Droplets by Electrowetting-based Actuation. *Proc. IEEE Micro Electro Mech. Syst.* **2002**, 32−35.
(27) Mach, P.; Krupenkin, T.; Yang, S.; Rogers, J. A. *Appl. Phys. Lett.* **2002**, *81*, 202.
(28) Hsieh, J.; Mach, P.; Cattaneo, F.; Krupenkin, T.; Yang, S.; Baldwin, K.; Rogers, J. A. *IEEE Photon. Technol. Lett.* **2003**, *15*, 81.
(29) Krupenkin, T.; Yang, S.; Mach, P. *Appl. Phys. Lett.* **2003**, *82*, 316.
(30) Yang, S.; Krupenkin, T.; Mach, P.; Chandross, E. A. *Adv. Mater.* **2003**, *15*, 940.

10.1021/la036093q CCC: $27.50
Published on Web 00/00/0000 PAGE EST: 3.8

in the droplet mobility. To achieve this kind of transition, we have developed a new method of applying electrowetting to nanostructured surfaces, where electrowetting is used to control the "local" contact angle, or the angle the liquid−air interface forms with the nanosize features of the surface. We have also observed similar transitions induced by changes in the liquid surface tension.

Wetting of Tunable Nanostructured Surfaces: Qualitative Description

The nanostructured superhydrophobic surfaces that we employed were constructed by etching a microscopic array of cylindrical nanoposts into the surface of a silicon wafer;[35] see Figure S1 (Supporting Information). Each post had a diameter of about 350 nm and a height of about 7 μm. The distance between posts (pitch) varied from 1 to 4 μm. An oxide layer was thermally grown to provide electrical isolation between the substrate and the liquid. A thin conformal layer of a low-surface-energy polymer was then deposited to create the hydrophobic surface. Materials and Methods (available in Supporting Information) contains a detailed description of the structures and how they were fabricated.

It is well-known that the contact angle of the liquid droplet on a smooth, unstructured surface is usually a monotonic function of the liquid surface tension.[31] As a part of our investigation, we wanted to determine whether our nanostructured surfaces would exhibit the same type of behavior. Several types of liquids were investigated, including water, alkanes, alcohols, ionic liquids, and various mixtures of these. As with planar surfaces, we observed that the contact angle primarily depended on the surface tension of the liquid and not on the specific type of liquid, but unlike the case with smooth surfaces, the contact angle of the nanostructured surfaces exhibited abrupt jumps to three different states; see Figure S2 (Supporting Information). For high-surface-tension liquids [such as water, surface tension 72 mN/m, or molten salt (1-ethyl-3-methyl-1*H*-imidazolium tetrafluoroborate), 62 mN/m], the droplet formed a highly mobile[32] ball with the contact angle $\theta \sim 180°$; see Figures 1a and S1a,b. For liquids with lower surface tensions (such as cyclopentanol, 33 mN/m, and octanol, 28 mN/m) the droplet underwent a transition to a completely immobile[32] state with a much smaller contact angle, see Figures 1c and S2c,d. Finally, for liquids with even lower surface tensions (such as 2-propanol, 24 mN/m, and methanol, 23 mN/m), the droplet appeared to completely wet the substrate; see Figure S2d.

Although the use of surface tension to induce transitions provides a valuable insight into the physics of the wetting phenomenon, practical applications are limited because the surface tension of the liquid cannot be substantially adjusted without changing the composition of the liquid. In many practical applications, it would be desirable to keep both the solid substrate and the composition of the liquid unchanged. To achieve this, one can use electrowetting instead of the surface tension to control the contact angle of the liquid on the substrate.[22−30] By applying a constant voltage (V) between the droplet and the silicon substrate, the cosine of the local contact angle θ_0, which the liquid forms with the walls of the nanoposts (see Figure S3), can be increased linearly with V^2.

In this work, two groups of liquids were investigated: high-surface-tension liquids (such as water and molten salt) and low-surface-tension liquids (such as cyclopentanol and octanol). A small amount of salt (such as potassium chloride or molten salt, approximately 0.01 M) was added to the liquids to provide sufficient electrical conductivity. Typical results (see Figure 1) are illustrated using molten salt and cyclopentanol as examples. With no voltage applied, a droplet of molten salt formed a highly mobile ball; see Figure 1a. With the application of about 22 V, the droplet underwent a sharp transition to the immobile droplet state; see Figure 1b. In comparison, with no voltage applied, a droplet of cyclopentanol formed an immobile droplet; see Figure 1c. As the applied voltage exceeded about 20 V, the contact angle dramatically decreased and the cyclopentanol droplet eventually filled most of the available substrate area; see Figure 1d. The details of the transition dynamics are clearly demonstrated in the video clips S1−3, which show the state of the droplet as a function of the applied voltage (available in Supporting Information).

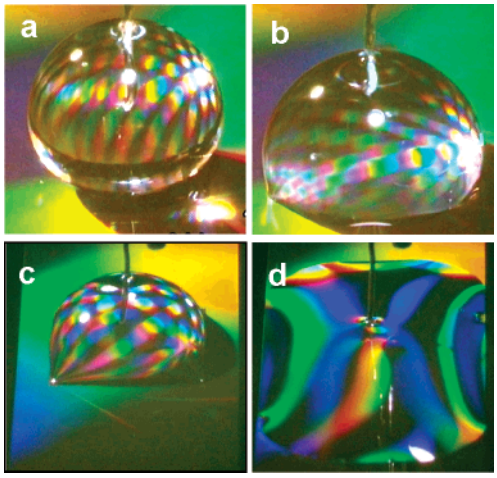

Figure 1. Four frames from the video recording demonstrating electrically induced transitions between different wetting states of a liquid droplet on the nanostructured substrate. The voltage was applied between the droplet (contacted through the Pt wire) and the substrate. (a) With no voltage applied, a droplet of molten salt formed a highly mobile ball on the 4-μm pitch substrate. (b) With the application of about 22 V, the droplet of molten salt underwent a sharp transition to the immobile droplet state. (c) With no voltage applied, a droplet of cyclopentanol formed an immobile droplet on the 1.75-μm pitch substrate. The unusual "square" shape of the base of the droplet reflects the underlying symmetry of the nanopost array. (d) With the application of about 50 V, the contact angle of the cyclopentanol droplet dramatically decreased and the droplet filled most of the substrate area.

To understand the microscopic nature of these transitions and, in particular, the degree of penetration of the liquid in the nanostructured layer, a UV polymerizable monomeric liquid (NA72, Norland, Inc., surface tension 40 mN/m) was employed. After dispensing on the substrate, the NA72 droplet was polymerized in situ by UV irradiation. The silicon substrate was then carefully broken, and the bottom of the solidified droplet as well as the delaminated complementary piece of the substrate were investigated using scanning electron microscopy.

For the rolling ball state (Figure 2a), there was no penetration of liquid in the nanostructured layer. The bottom of the droplet showed clear imprints of the tips of the nanoposts, but there were no signs of nanoposts embedding into the polymer. It was a completely different case for the immobile droplet (Figure 2b), where the liquid clearly penetrated all the way to the bottom of the nanostructured layer, dramatically increasing the area

(31) de Gennes, P. G. *Rev. Mod. Phys.* **1985**, *57*, 827.
(32) The procedure used to determine the droplet mobility is outlined in Materials and Methods available in Supporting Information.

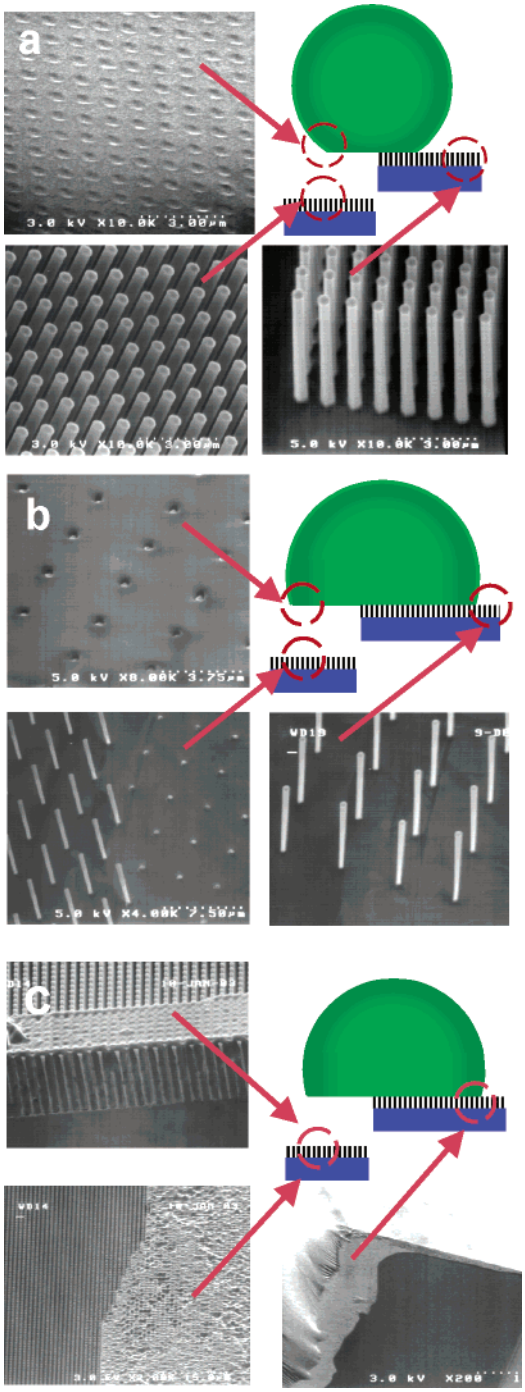

Figure 2. Scanning electron micrographs of solidified in situ droplets of NA72. (a) The rolling ball state showed no penetration of liquid though the nanostructured layer. The bottom of the droplet showed clear imprints of the nanopost tips, but no penetration into the liquid. All the nanoposts on the delaminated piece of the substrate were undamaged. (b) Immobile droplets exhibited complete penetration of the liquid through the nanopost array. All the nanoposts underneath the droplet were embedded in the liquid and broken at their bases upon delamination from the substrate. No damage to the nanoposts located outside the droplet was observed. (c) The droplet solidified during the electrowetting process. The resulting immobile droplet exhibited complete penetration of the liquid through the nanopost array. The droplet was preceded by a precursor layer, which was formed by the liquid wetting the nanopost array.

of the liquid−solid interface. Thus, the transition between the rolling ball state and the immobile droplet state was accompanied by the penetration of liquid in the nanostructured layer. A similar investigation showed that the electrowetting-induced transition between the states of the droplet was also accompanied by the liquid penetrating through the nanostructured layer, as seen in Figure 2c.

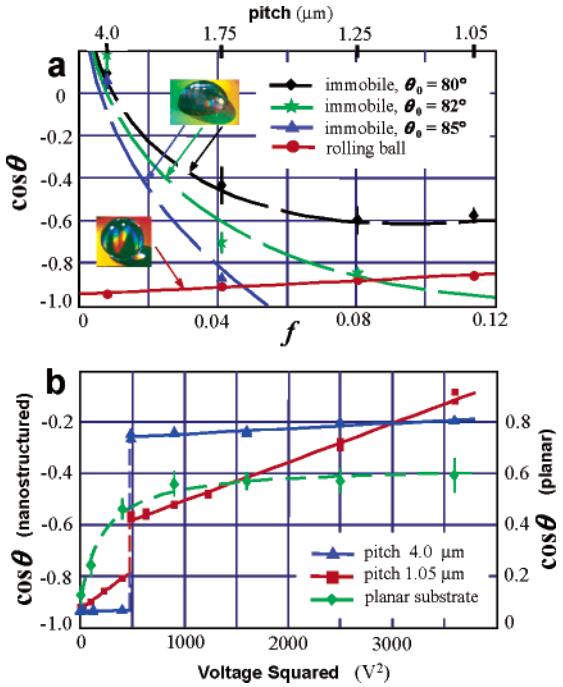

Figure 3. Contact angle θ of the droplet as a function of the applied voltage and the areal density of nanoposts f. (a) cos θ as a function of f for 30, 40, and 50% methanol−water mixtures (contact angle on the planar substrate θ_0 = 85, 82, and 80°). The rolling ball states are shown as one curve because of the scale of the figure. The red line represents the best linear fit, while the blue, green, and black lines are to guide the eye only. The vertical lines represent standard deviation. (b) cos θ as a function of applied voltage squared for the molten salt on the nanostructured and planar substrates. The solid lines represent the best linear fit, while the dashed lines are to guide the eye only. The vertical lines represent standard deviation.

Wetting of Tunable Nanostructured Surfaces: Contact Angle Behavior

To achieve a better quantitative understanding of the droplet behavior, the apparent contact angle θ was measured on each of the four nanostructured substrates. By apparent contact angle we mean the macroscopically observed advancing contact angle that the liquid forms with the plane perpendicular to the nanoposts. Additionally, an advancing contact angle was measured on an identically treated planar substrate. The latter measurement was performed to obtain an estimate of the value of the local contact angle θ_0 that the liquid forms with the walls of the nanoposts. It should be noted that the values of θ_0 obtained in this way should be treated as an estimate only, mostly illustrating relative changes in θ_0 rather than the actual value itself. The contact angle measurement procedure, including error analysis, along with the equipment used is described in detail in Materials and Methods (available in Supporting Information).

First, the value of the apparent contact angle was measured as a function of the liquid surface tension. Methanol−water mixtures with increasing volume concentrations of methanol were used to obtain a sequence of liquids with progressively decreasing surface tensions. One can see (Figure 3a) that the contact angles θ for the rolling ball state and for the immobile droplet state show very different behaviors as a function of the areal density

of posts (which is represented as $f = \pi d^2/(4l^2)$—the fraction of the area covered by the post tips—see Materials and Methods, Supporting Information). For the rolling ball state, cos θ increased linearly with f, a behavior that is in agreement with the well-known Cassie and Baxter equation[2]

$$\cos \theta = f(\cos \theta_0 + 1) - 1 \quad (1)$$

where θ_0 is the local contact angle. A small vertical offset for the cos θ versus f curve in Figure 3a can be easily explained by the influence of gravity on the droplet shape. If the value of θ_0 is calculated using the Cassie and Baxter equation, $\theta_0^{(t)} \approx 105°$ is obtained, which is about 25% above the value estimated from the contact angle on the planar substrate. For the case of the immobile droplet, a rapid nonlinear decrease of the cosine of the contact angle θ with the increase in the areal density of posts f (see Figure 3a) was observed. This type of behavior is directly the opposite of what would be expected based on the Cassie and Baxter approach.

Several physical phenomena can account for the observed behavior. Contact line tension[31,33,34] is known, both from theory and from experiment, to contribute substantially to the contact angle behavior at the scale below tens of micrometers. Thus, one might expect that the line tension would affect the observed droplet behavior, especially with respect to the values of the local contact angle.

Another important consideration is whether the droplet can attain thermodynamic equilibrium after undergoing the transition. One could expect that the dynamic effects, such as contact angle hysteresis, associated with the liquid propagating through the nanostructured layer, might prevent the droplet from doing so. In this case, the observed contact angle θ becomes essentially a dynamic property of the system. As such, it should be described by the model that reflects the kinetics of the system, such as the kinetics of the liquid front moving through the wetted nanostructured layer.

To quantitatively investigate electrowetting-induced transitions, the apparent contact angle of the molten salt on all four nanostructured substrates, as well as on an identically treated planar substrate, was measured as a function of the applied voltage. The contact angle of the droplet on a nanostructured substrate appeared to follow typical electrowetting behavior[22−24] with cos θ proportional to V^2; see Figure 3b. However, it showed no saturation for the whole range of investigated voltages in contrast to a rapid saturation on an identically treated planar substrate see Figure 3b).

Experimental data clearly indicate (Figure 3b) a sharp transition from a rolling ball state to an immobile droplet state at about 22 V. This corresponds to a local contact angle of 110° estimated from our experimental data, which compares well to $\theta_0^{(t)} \approx 105°$, the angle that corresponds to a transition induced by changes in the surface tension and calculated from the Cassie and Baxter equation, as discussed earlier. The present data clearly indicate a close connection between electrowetting-induced and surface-tension-induced transitions. A detailed theoretical model describing the dependence of the contact angle on the applied voltage and liquid surface tension is currently under development and will be discussed in a separate publication.

Conclusions

In this work, a new method of dynamic electrical control over the wetting behavior of liquids on the nanostructured superhydrophobic surfaces is proposed and experimentally demonstrated. The method relies on using electrowetting to adjust the local contact angle that the liquid forms with the nanosized features of the surface. The widest possible tunability range, from strong superhydrophobic behavior to nearly complete wetting, has been achieved.

The contact angle on these surfaces was studied and found to exhibit abrupt transitions to three different states as a function of the applied voltage and liquid surface tension. The microscopic nature of these transitions and, in particular, the associated penetration of the liquid in the nanostructured layer was experimentally investigated.

The ability to dynamically change the interaction between the liquid and the nanostructured substrate potentially opens a wide range of exciting new applications. The particular areas of interest include microfluidics, lab-on-a-chip devices, chemical microreactors, thermal management of microelectronics, drag reduction systems, and optical communications, as well as many others.

In conclusion, the authors hope that the reported results on the dynamically tunable nanostructured superhydrophobic surfaces will provide a new insight into the physics of liquid−solid interfaces as well as further stimulate the development of novel applications.

Acknowledgment. Discussions with Avi Kornblit, Warren Y.-C. Lai, Ray Cirelly, Mary Mandich, Alan Lyons, Lou Manzione, Cherry Murray, and David Bishop are greatly appreciated. Also appreciated was the processing support from the New Jersey Nanotechnology Consortium. T.M.S. acknowledges the support of the Studienstiftung des deutschen Volkes.

Supporting Information Available: Materials and Methods, Figures S1−3 (as described in the text), and Movies S1−3. This material is available free of charge via the Internet at http://pubs.acs.org.

LA036093Q

(33) Widom, B. *J. Phys. Chem.* **1995**, *99*, 2803.
(34) Aveyard, R.; Clint, J. H. *J. Chem. Soc., Faraday Trans.* **1996**, *92*, 85.
(35) McAuley, S. A.; Ashraf, H.; Atabo, L.; Chambers, A.; Hall, S.; Hopkins, J.; Nicholls, G. *J. Phys. D: Appl. Phys.* **2001**, *34*, 2769.